LBT

PULTRUDED STRUCTURAL SHAPES - FROM THE CONSTITUENTS TO THE STRUCTURAL BEHAVIOR

Ever J. Barbero
Constructed Facilities Center, Department of Mechanical and Aerospace Engineering, West Virginia University, Morgantown, WV

ABSTRACT

This paper addresses the prediction of engineering properties of pultruded structural shapes (e.g., EXTREN™), PULTREX™) based on the processing description used by the pultrusion industry. Since the strength-to-stiffness ratio of composites is much larger than that of steel or concrete, deflections are of major concern to the structural designer. In this paper, it is shown how to predict axial, bending, and shear stiffnesses of the structural shapes based on the fiber and resin properties and their arrangement in the cross section. Correlations between properties predicted by this method and measured by full size testing of commercially available structural shapes (PULTREX™) are shown. Intermediate steps in the analysis by comparison to material testing data from samples of the same pultruded section were validated. This work also serves as the basis for more complex analysis of the behavior of pultruded structural shapes that are addressed in companion papers. Recommendations as to how the pultrusion industry may use this model to optimize the performance of new structural shapes are presented.

INTRODUCTION

Cooling towers, antenna enclosures, chemical plant structures, and other applications (1-4) show the usefulness of pultruded structural members. Advanced composite beams and columns have been used successfully by the aerospace industry over the years (5-7). Recent advances in pultrusion process modelling (8-9) and control (10) anticipate improved quality on a variety of larger shapes pultruded with new fiber and resin systems.

Composite materials have many advantages over conventional construction materials like steel and reinforced concrete. Light weight, corrosion resistance, lower installation cost, no electromagnetic interference, are a few examples. Most prominent is the possibility of creating the best material for each particular application. The full potential of composites cannot be realized unless the material is designed concurrently with the structure. An example of such an approach is the design of structures with reinforced concrete. However, composites give much more latitude to the designer. In this work we develop some of the tools required to perform such a concurrent design of the material tailored for the specific application at hand.

Characteristics of interest to the structural engineer are stiffness, strength, buckling resistance, etc. These structural properties depend of the material system (composite) and the shape of the cross section of the members, which are variables controlled by the manufacturer. As with steel I-beams, the shape can be optimized to increase the bending stiffness without compromising the maximum bending strength. In contrast to steel, with composite beams, we can optimize the material itself by choosing among a variety of resins, fiber systems, and fiber orientations. Changes in geometry can be easily related to changes in the bending stiffness through the moment of inertia. However, changes in the design of the material do not produce such an obvious result because composites have properties that depend on the orientation of the fibers, the fiber volume fraction, etc.

The strength-to-stiffness ratio of composites is much larger than that of steel or concrete. Therefore, deflections usually control the design with composite structural shapes. Axial stiffness governs the design of trusses, stay cables, etc. Bending stiffness and shear stiffness control the bending behavior of beams. Shear deformation plays a significant role in the transverse deflection of composite beams. Although the stiffness of existing pultruded members can be measured experimentally, the analytical prediction of stiffnesses from the properties of the material constituents allows optimizing of the structural shapes (11). The model presented will predict buckling (12) and bending strength (13).

This paper addresses the prediction of stiffness properties from the product description used for manufacturing. This includes the material properties of the constituents (fiber and matrix), the orientation and volume fraction of the fibers at different locations on the section (web or flanges), and the shape of the cross section. Data is provided to favor a laminated idealization of pultruded materials.

MODELING OF PULTRUDED STRUCTURAL SHAPES

Fiber reinforced composite beams and columns are inhomogeneous for two reasons. First, the fiber reinforced composite material is inhomogeneous and anisotropic due to the presence of the fiber (glass, kevlar™, graphite). Second, different portions of the cross section are built with different orientation of the fibers, different fiber volume fractions, different fiber systems, etc. The inhomogeneity is evident not only from one point to another in the material (e.g., roving, nexus, continuous strand layers) but also at a macroscopic scale, since, for example, the flanges and webs are usually built with different fiber combinations.

Although pultruded beams are not manufactured by lamination, they do contain different material combinations through the thickness, thus justifying the use of lamination theory. Micromechanics is employed to model each layer as a homogeneous equivalent material behaving macroscopically similar to the fibrous composite (Section 3.1). Next, lamination theory (Section 3.2) is used to model an entire flange or web again as an equivalent homogeneous material. Finally, flanges and webs are assembled into a structural shape (Section 3.3) to obtain useful structural design properties.

Micromechanical Model for Pultruded Composite Beams

By using micromechanics the material properties for a lamina ($E_1, E_2, \nu_{12}, G_{12}$) are determined from the material properties of the fiber (E_f, ν_f) and the matrix (E_m, ν_m). The elasticity approach to micromechanics seems to provide the best predictions for pultruded composite materials.

In the elasticity solutions with contiguity, it is assumed that either a) fibers are contiguous (i.e., fibers touch each other) or b) fibers are isolated (i.e., fibers are completely separated by resin). If C denotes the degree of contiguity, then C=0 corresponds to isolated fibers and C=1 corresponds to perfect contiguity. For pultruded composites with low fiber volume fraction, C=0 is used. Due to the high tension that pultrusion exerts on the fibers, a fiber misalignment factor K=1 has been adopted. Using Eqs. 3.69, 3.66, and 3.67 from Ref. (14), we obtain the material properties of each lamina (E_1, E_2, and ν_{12}).

The fiber volume fraction V_f is the ratio of the volume of fiber to the total volume of the final product. V_f has been calculated as the quotient of the area of fibers in the cross section to the total area of the cross section. The area A of fibers in the cross section depends of the number of rovings n, and their yield y 0.9144 m (number of yards) of roving weighing 0.454 kg (1 lb), and their density. Finally, the area as $A = n(2.016\, y\, \rho)$, with A in m^2, ρ in kg/m^3, and y in (yards/lb) is computed.

For the determination of the shear modulus, we use the elasticity solutions with contiguity ((14), Eq. 3.68). The predicted value did not correlate well with experimental data (15), and the experimental value was used instead in our analysis. Currently improved micromechanical models are being investigated for shear of pultruded composites.

Macromechanical Model of Pultruded Structural Shapes

The kinematic equations for laminated composite beams used in this work are those of Timoshenko's beam theory (!6). In this theory, the constitutive equations of a composite beam with thin laminated flanges are developed under the assumption that the following stress components are negligible (Figure 1).

$$\sigma_z \approx \sigma_y \approx \sigma_{yz} \approx \sigma_{xy} \approx 0 \qquad [1]$$

Therefore, the material constitutive equations are

$$\begin{aligned} \sigma_x &= E_x \epsilon_x \\ \sigma_{xz} &= G_{xz} \gamma_{xz} \end{aligned} \qquad [2]$$

where E_x is the equivalent axial stiffness and G_{xz} is the equivalent shear stiffness of the material. For an isotropic material, the modulus of elasticity $E_x=E$, and the shear modulus $G_{xz}=G$. E_x and G_{xz} are apparent properties in the *structural* coordinate system (Figure 1). By *rotation* from the material coordinate system (Figure 2) to the *structural* coordinate system, we obtain

$$E_x = \overline{Q}_{11} + \overline{Q}_{12}\frac{\overline{Q}_{16}\overline{Q}_{26} - \overline{Q}_{12}\overline{Q}_{66}}{\overline{Q}_{22}\overline{Q}_{66} - \overline{Q}_{26}^2} + \overline{Q}_{16}\frac{\overline{Q}_{26}\overline{Q}_{12} - \overline{Q}_{22}\overline{Q}_{16}}{\overline{Q}_{22}\overline{Q}_{66} - \overline{Q}_{26}^2} \qquad [3]$$

and

$$G_{xz} = -\frac{\overline{C}_{45}^2}{\overline{C}_{44}} + \overline{C}_{55} \qquad [4]$$

for the flange (Figure 2) and

$$G_{xz} = \overline{Q}_{66} \qquad [5]$$

for the web (Figure 3), where the *over-line* indicates a *rotated* quantity (14). Here, $\overline{Q}_{ij}$ ((14), Eq. 2.80 and 2.62) and $\overline{C}_{ij}$ ((15), Eq. 4.3.14) are the lamina stiffness, which are a function of the lamina material properties. E_1 is the modulus of elasticity along the fiber direction (Figure 2). E_2 is the modulus of elasticity in the direction perpendicular to the fibers. G_{12} is the shear modulus in the plane of

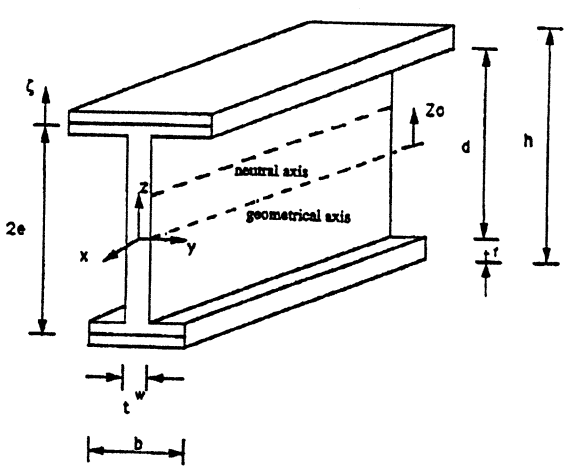

Figure 1. Typical structural shape and coordinate system.

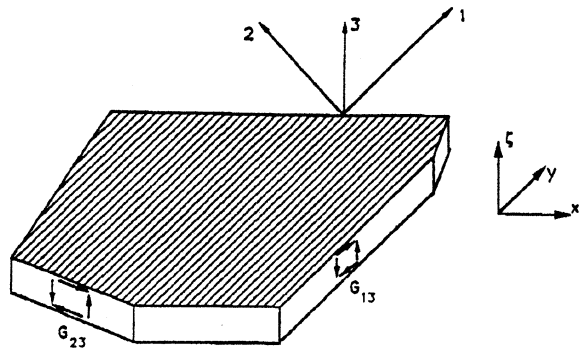

Figure 2. Typical flange lay-up and coordinate system.

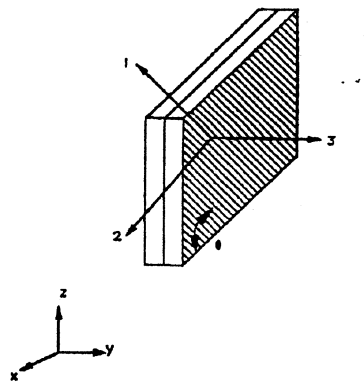

Figure 3. Typical web lay-up and coordinate system.

the laminate and G_{23} the out-of-plane shear. Each layer is assumed to be transversely isotropic (14). Therefore, $E_3=E_2$ and $G_{13}=G_{23}$. As an example, if $\theta=0$ then $E_x=E_1$. Similarly if $\theta=\pi/2$ then $E_x=E_2$.

The constitutive equations of a laminate (flange or web), the so called *laminate constitutive equations,* are derived by integrating the expression of the stress resultants N_x, M_x, and Q_x as a function of the in-plane strains ϵ^0_x, curvature κ_x, and shear strain γ_{xz} to give

$$\begin{aligned} N_x &= A\epsilon_x^0 + B\kappa_x \\ M_x &= B\epsilon_x^0 + D\kappa_x \\ Q_x &= F\gamma_{xz} \end{aligned} \qquad [6]$$

where **A** is the extensional stiffness, **D** is the bending stiffness, **F** is the shear stiffness, and **B** is the bending-extension coupling for unsymmetrical laminates. For the flange, the following equations hold

$$\begin{aligned} A^f &= b \sum_{k=1}^{N^f} E_x^k t_k \\ B^f &= b \sum_{k=1}^{N^f} E_x^k t_k \bar{\xi}_k \\ D^f &= b \sum E_x^k \left(t_k \bar{\xi}_k^2 + \frac{t_k^3}{12}\right) \\ F^f &= b \sum_{k=1}^{N^f} G_{xz}^k t_k \end{aligned} \qquad [7]$$

where ξ is a local coordinate attached to the flange (Figure 1), $\bar{\xi}$ is the position of the middle surface of the k-th layer in the local coordinate system, b is the width of the flange, and N^f is the number of layers of the flange. G^k_{xz} is the out-of-plane shear modulus of the k-th layer in the flange (Eq. 4). For the web, the following equations hold

$$\begin{aligned} A^w &= d \sum_{k=1}^{N^w} E_x^k t_k \\ B^w &= 0 \\ D^w &= \frac{d^3}{12} \sum_{k=1}^{N^w} E_x^k t_k \\ F^w &= d \sum_{k=1}^{N^w} G_x^k t_k \end{aligned} \qquad [8]$$

where d is the depth of the web and N^w is the number of layers of the web. G^k_{xz} is the in-plane shear modulus of the k-th layer in the web (Eq. 5).

Beam Stiffness

To obtain the stiffness of the whole section, the contribution of the flanges (Eq. 6) and the webs (Eq. 7) is combined using the parallel axis theorem ((18), Section 6, Chapter 6) with respect to the axis of symmetry of the cross-section.

$$\begin{aligned} A &= 2A^f + A^w \\ B &= e(A^{top} - A^{bot}) + B^{top} + B^{bot} \\ F &= F^w \end{aligned} \qquad [9]$$

Note that the contribution of the flanges to the shear stiffness is omitted in Eq. 9. For unsymmetrically laminated beams, we compute the location of the neutral axis is computed as

$$z_0 = \frac{B}{A} \qquad [10]$$

Next, we compute the bending stiffness D with respect to the neutral axis using the parallel axis theorem (Figure 1) as

$$\begin{aligned} D = D^{web} + D^{top} + D^{bot} + A^{top}(e - z_0)^2 \\ - A^{bot}(e + z_0)^2 + A^{web} z_0^2 \end{aligned} \qquad [11]$$

This completes the prediction of structural properties from the basic information about the composition of the pultruded structural shape. While our analysis is general, it coincides with the three-dimensional elasticity solution for the particular case of laminated beams with transversely isotropic lamina (19). Based on the exact elasticity solution, Chen (19) concludes that Euler-Bernouli beam theory yields excellent results for normal stress at the i-th layer using

$$\sigma_i = \frac{M z E_i}{\sum_j E_j (I_{yy})_j} \quad [12]$$

and transverse deflections using

$$\sum_i E_i (I_{yy})_i \quad [13]$$

instead of **EI** in the flexure formula. Unlike our analysis, Chen (19) is not concerned with monoclinic lamina (i.e., off-axis fiber reinforced composite lamina) in complex pultruded shapes nor with the problem of low shear modulus. In this paper, we generalize Eq. 13 for arbitrarily laminated beams, calling it *bending stiffness* **D**, and propose its use in the deflection formula of Timoshenko's beam theory. A general procedure for the computation of stresses that resembles and generalizes Eq. 12 is presented in Ref. 20.

APPLICATION TO CURRENT STRUCTURAL SHAPES

As an example, consider a pultruded 20.3 x 20.3 cm (8" x 8") wide-flange I-beam of E-Glass-Vinylester composite. A typical layer has 20 roving of 61 yield distributed over 2.5 cm^2 (1.25 mm thick by 20.3 cm wide) of the flange. Following Section 3.1, this layer has a fiber volume fraction V_f = 0.25. For the material under study, we use: E_f = 72.349 GPa, E_m = 3.378 GPa (21) and $\nu_f = 0.22$, $\nu_m = 0.335$ (14). Using the elasticity approach, we obtain: E_1 = 20.632 GPa, E_2 = 4.872 GPa, $\nu_{12} = 0.313$, and G_{12} = 1.986 GPa.

All the layers are next considered in the flange and web according to the processing specifications used by the pultrusion manufacturer. Using the macro mechanical analysis of Section 3.2, we obtain the following values: the equivalent modulus of elasticity for the flange is E_x = 20.5 GPa which compares very well with the experimental value of E_x = 20.2 GPa (15); the equivalent modulus of elasticity for the web is E_x = 15.9 GPa which compares very well with the experimental value of E_x = 15.2 GPa (15).

The stiffness of the whole section is computed following Section 3.3 and obtains a bending stiffness of the beam D = 761.1 KNm^2 as obtained in Ref. (13) following the procedure introduced by Ref. (22). This value, along with the shear stiffness F, can be used directly in the equations for deflections derived from Timoshenko's beam theory (16).

BUCKLING AND CRIPPLING ANALYSIS

Common structural columns have open or closed sections of thin composite walls. Column buckling and crippling are the main considerations in their design. In this section, we present design charts with failure envelopes for different buckling modes of some commercially available structural shapes along with selected experimental data for comparison of predicted and observed behavior. Micromechanical models and lamination theory are utilized to model the pultruded composite material along the lines of Sections 3.1 and 3.2.

For long columns, the Euler equation is modified to account for the anisotropic nature of the material. For intermediate column lengths, local buckling occurs first, which triggers the global buckling of the column. For short columns, material crushing occurs, possibly preceded by micro-buckling of the fibers in the composite. Using the results of Section 3, the long column buckling problem can be easily solved replacing the modulus of elasticity E by the bending stiffness D in the equations presented in Refs. (12,23):

$$P^{cr} = \frac{\pi^2}{L^2} D \quad [12]$$

Local buckling occurs on the compression flange of box- and I-beams in bending or in columns under axial compression. The flanges can be modelled as a plate elastically supported by the webs (and possibly free at the edges, depending of the shape of the section). The elastically clamped edge can be modelled (12) as: flexible flange-web connection, rigid flange-web connection, or hinged flange-web connection.

Figure 4 shows local and global buckling loads for a 15 x 15 cm (6" x 6") I-beam as a function of the length of the column. For a short length, the flanges buckle in mode one (m=1). The critical load reaches a minimum for a length of 15 cm. For a longer length, the mode number increases but the minimum critical load is constant. This implies that the local buckling of the flanges is independent of the length of the beam and only dependent on the axial load applied, which agrees with the observed behavior in the full scale experimental program. The predicted wave length of 15 cm agrees with the measured wave length (Figure 5) of 15 cm for an I-beam in bending. In Figure 6, the local and global buckling load for a 10 x 10 cm (4" x 4") box-beam as a function of the length of the column is shown.

As it is demonstrated by the experiments reported in Ref. (13), local buckling of the compression flanges initiates a process that leads to the collapse of the member. Predic-

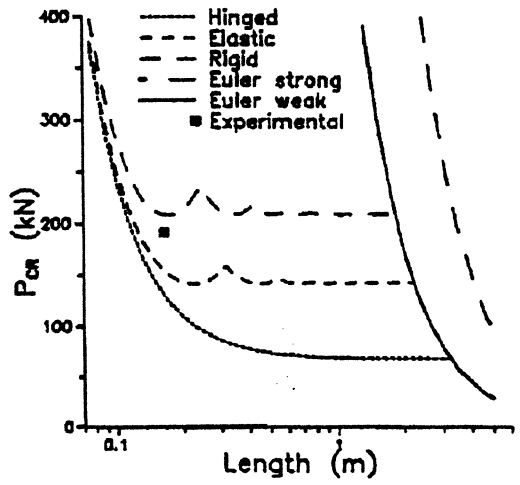

Figure 4. Failure envelope for an I-beam.

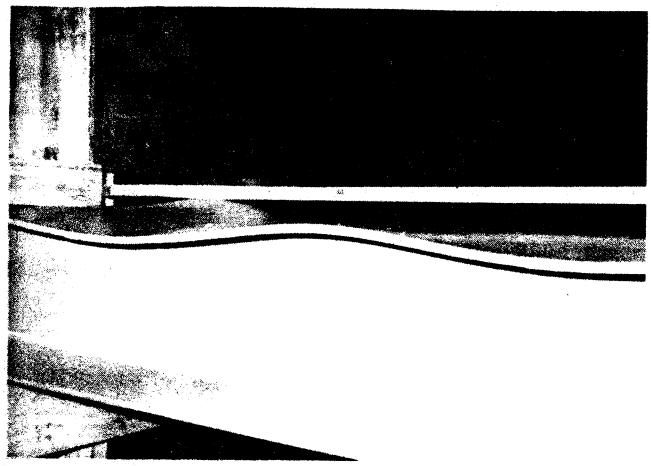

Figure 5. Post-buckling shape of the top flange of an I-beam.

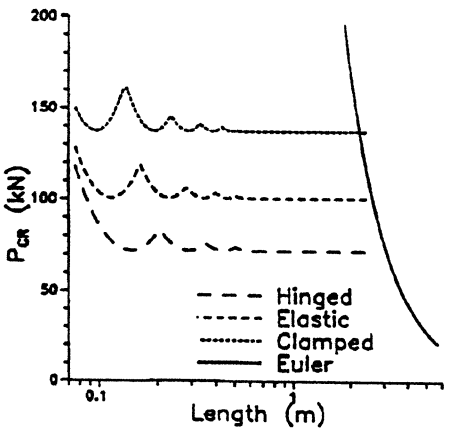

Figure 6. Failure envelope for a box-beam.

tion of local buckling is therefore crucial for the prediction of ultimate bending strength of the pultruded beams in bending. Also, local buckling precipitates global (Euler) column buckling for columns of intermediate length. Therefore, it is possible to increase the bending strength and column buckling resistance of pultruded structural shapes by optimizing the material system.

OPTIMIZATION OF THIN-WALLED COMPOSITE SECTIONS

Experimentally, it was observed (Figure 5) that the compression flange of composite beams buckle in local modes when the beam is subjected to bending. The post-buckling deformations are large, which precipitate failure. Buckling of the compression flange was the first failure event on the three-point bending testing of several sizes of I-beams of various lengths. The prediction of material properties and the buckling analysis presented in Ref. (12) has been correlated experimentally only for laminates with 0° roving, nexus, and continuous strand layers. The model is applied in this section to other lamination schemes where the 0° layers remain unchanged (Figures 7 and 8). The thicknesses previously occupied by nexus and continuous

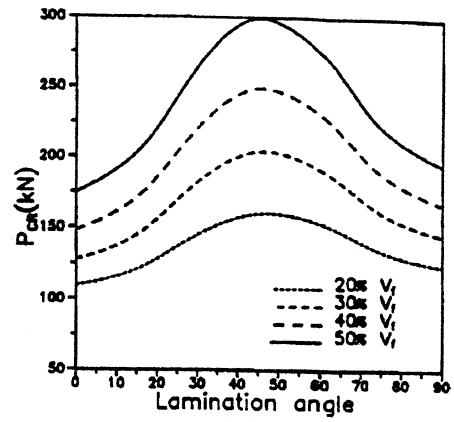

Figure 7. Optimization of the lamination angle for an I-beam.

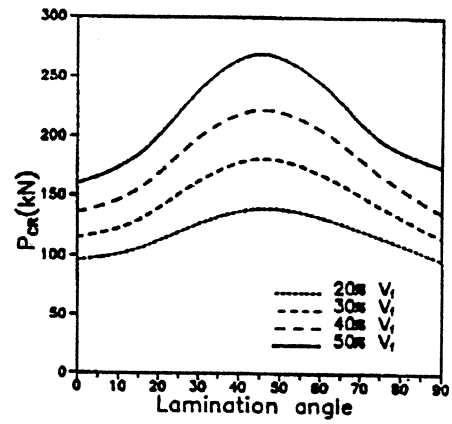

Figure 8. Optimization of the lamination angle for a box-beam.

strand are replaced by angle ply layers. Since actual fiber volume fraction achievable with angle ply layers in the pultrusion process is not known, results for several volume fractions from 20% to 50% are shown in Figures 7 and 8. The fiber volume fraction of the 0° layers represents the actual value of currently produced sections. Figure 7, for a box-beam with elastic flange-web connections, indicates that, according to this model, a [±45°] lamination gives the largest critical load possible regardless of the fiber volume fraction. Either 0° or 90° lamination gives the lowest possible critical load for the buckling of the compression flange. Figure 8, for an I-beam with elastic flange-web connection, indicates the same trend..

CONCLUSIONS

This paper presents a complete, step by step, predictive analysis of the stiffness properties of pultruded structural shapes. The method starts with the process description of the pultruded shape used by the pultrusion manufacturer and successfully predicts the properties of interest to the structural designer. Predicted properties for a

PULTREX™ structural shape coincide with full size test results. Intermediate results also correlate well with coupon testing on the same material. This is the first comprehensive treatment of the prediction of structural properties available to the pultrusion manufacturer. As such, it is useful for development of new structural shapes or improvement of existing ones. It is also useful for estimation of structural properties of a large variety of existing structural shapes, for which, a comprehensive experimental program may prove to be an extenuating task. However, a selective experimental program may serve to further validate and/or improve the methodology presented in this paper. The tools presented in this paper are also useful for the prediction of strength, buckling, and crippling, which are briefly presented here. The stiffnesses predicted by the methodology of this paper are directly applicable to structural design with pultruded structural shapes.

ACKNOWLEDGEMENTS

The author wishes to thank Dr. Hota GangaRao, Director of the Constructed Facilities Center at West Virginia University for providing valuable suggestions to this work. Helpful comments on this research paper by Dr. Julio Davalos are deeply appreciated. The contributions of the graduate students and staff involved in this project are also recognized. This research was performed under NSF Grant 8802265 and WVDOH Grant RPT699. The financial support is gratefully acknowledged.

REFERENCES

1. C. Ballinger, "Structural FRP Composites", Civil Engineering, 63-65, July, 1990.
2. P.R. Evans and J.M. Slepetz, *Proceedings of the 4th Conference on Fibrous Composites in Structural Design,* 1978, pp. 687-700.
3. A. Green, "Glass Fiber Reinforced Composites in Building Construction:, Transportation Research Record 1118, 73-76, Transportation Research Board, National Research Council, Washington, DC, 1987.
4. B.S. Thompson, *Applied Mechanics Review,* **40**(11), 1545(1987).
5. D.L. Bonanni, E.R. Johnson and J.H. Starnes Jr., *Proceedings 29th SDM Conference,* 1988, AIAA Paper 88-2251, pp. 313-323.
6. D.H. Hodges, *Proceedings 29th SDM Conference, ibid,* AIAA Paper 88-2249, pp. 305-312.
7. L.W. Rehfield, A.R. Atilgan and D.H. Hodges, *ibid,* AIAA Paper 88-2250.
8. G.L. Batch and C.W. Macosko, *Proceedings of ASME Manufacturing International '88,* **4,** 1988, pp. 57-62.
9. E.J. Barbero and G. Krishnan, "Eulerian Finite Element Formulation of the Fluid Mechanics in the Pultrusion Process", *32nd SDM Conference,* April 8-10, Baltimore, MD, 1991b.
10. S.C. Nolet and J.P. Fanucci, *Proceedings of the SPI Composites Institute 45th Annual Conference & Expo '90,* 1990, pp. 1-7.
11. E.J. Barbero, *International SAMPE Symposium and Exhibition,* **36,** (1991a).
12. E.J. Barbero and I. Raftoyiannis, "Buckling Analysis of Pultruded Composite Columns", *ASME Winter Annual Meeting,* 1990a.
13. E.J. Barbero and S.H. Fu, "Local Buckling as Failure Initiation in Pultruded Composite Beams", *ASME Winter Annual Meeting,* 1990b.
14. R.M. Jones, *Mechanics of Composite Materials,* Hemisphere Publishing Corporation, 1975.
15. E.J. Barbero and S. Sonti, "Micro Mechanical Models for Pultrded Composite Beams", *32nd SDM Conference,* April 8-10, Baltimore, MD, 1991b.
16. J.M. Gere and S.P. Timoshenko, *Mechanics of Materials,* 2nd Edition, PWS Engineering, Boston, 1984.
17. J.N. Reddy, *Energy and Variational Methods in Applied Mechanics,* John Wiley, New York, 1984.
18. S.W. Tsai and H.T. Hahn, *Introduction to Composite Materials,* Technomic Publishing Co., Lancaster, PA, 1980.
19. S. Cheng, X. Wei and T. Jiang, *ASCE J. Eng. Mech.,* **6,** 1150 (1989).
20. E.J. Barbero, "Beam Lamination Theory for Complex Structural Shapes", CFC Report, West Virginia University, August 1990c.
21. *Creative Pultrusions Design Guide,* Creative Pultrusions, Inc., Pleasantville Industrial Park, Alum Bank, PA 15521.
22. Y.M. Tarnopolskii and T. Kincis, *Static Test Methods for Composites,* translated from the third revised and supplemented Soviet Edition, George Lubin Ed., Van Nostrand Reinhold Co., New York, 1985.
23. D.O. Brush and B.O. Almroth, *Buckling of Bars, Plates, and Shells,* McGraw-Hill, New York, 1975.

BIOGRAPHY

Ever J. Barbero, a member of SAMPE® and ASME, graduated from Universidad Nacional de Rio Cuarto - Argentina with a BS in Electrical Engineering (1983) and a BS in Mechanical Engineering (1983). He was a Research Fellow at INTEC-Argentina from 1984 to 1986, and was awarded the Cunningham Dissertation Fellowship. In October of 1989, he received his Ph.D from Virginia Polytechnic Institute and State University. He is Assistant Professor of Mechanical and Aerospace Engineering at West Virginia University and also a member of the Constructed Facilities Center at WVU conducting research on the application and development of fiber reinforced composites for construction of large structures.